Astron. Astrophys. 339, 113–122 (1998)

ASTRONOMY AND ASTROPHYSICS

Using polarimetry to check rotation alignment in PMS binary stars

Principles of the method and first results⋆

J.-L. Monin[1,2], **F. Ménard**[1], **and G. Duchêne**[1]

[1] Laboratoire d'Astrophysique, CNRS UMR 5571, Observatoire de Grenoble, Université Joseph Fourier, BP 53, F-38041 Grenoble Cedex 9, France

[2] Institut Universitaire de France

Received 16 March 1998 / Accepted 27 August 1998

Abstract. We present a new method to use polarimetric measurements to estimate the relative orientations of the star+disk system in each component of Pre Main Sequence (PMS) T Tauri binary stars. The principles of the method are presented, together with a review of polarimetric data available in the literature on wide systems ($8-40''$) in Taurus. We show that this method can be subject to a bias introduced by the interstellar polarization, but we find that in four sources that are not affected by this bias, the rotation axes of both components are preferentially parallel. We also find one system where the axes are clearly *not* parallel. Because it concerns wide binaries, this alignment is thought to result from initial binary formation itself rather than via a posteriori tidal interactions. The method is promising but requires the use of more accurate polarimeters. In order to test the possibility to study tighter systems, we have also obtained imaging polarimetric measurements and spectra for each components of closer binaries ($< 3''.2$). Our first polarimetric measurements lack S/N, but the spectra of individual components of these close binaries provide information on their respective spectral types and their accretion rate through H_α equivalent widths and fluxes. We use these spectra to confirm the nature and the pairing tendency of the TTS under study. Implications on the binary formation mechanism are discussed.

Key words: techniques: polarimetric – techniques: spectroscopic – stars: pre-main sequence – stars: binaries: close – circumstellar matter

1. Introduction

Our current understanding of low mass stellar formation has to take into account two very different yet complementary constraints. On one hand, when we consider individual stars, the current model put forward for embedded Young Stellar Objects (YSOs) includes a central stellar core, surrounded by an equatorial accretion disk and a remnant infalling envelope (see e.g., Shu et al. 1987). This stage is frequently associated with energetic bipolar molecular outflows, perpendicular to the disk (e.g., Bachiller, 1996 and references therein) and tracing the symmetry axis of the whole system. Even if the circumstellar disk is warped by the influence of a close companion (see e.g., Terquem and Bertout, 1992), its axis remains very close to the star's rotation one.

On the other hand, we also know that a large fraction of T Tauri stars (TTS) form in binary or multiple ($N > 2$) systems (e.g., Ghez, et al. 1993; Simon et al. 1995; Ghez et al. 1997; Padgett et al. 1997). This ubiquitous property of the stellar formation process has a potentially enormous influence on the previous one because the circumstellar environment of the individual components of a multiple system can be deeply modified by the presence of a companion. For instance, in the case of a binary, the dust thermal continuum emission at millimeter wavelengths is smaller on average than for singles, indicating that the outer colder part of the circumstellar disks surrounding binary components have been removed, leading to a smaller reservoir of material immediately available for accretion (e.g., Osterloh & Beckwith 1995; Dutrey et al. 1996).

From the theoretical point of view, fragmentation now appears as the best binary formation mechanism to meet the observational constraints (Boss, 1993). Fragmentation mechanisms include fragmentation of a molecular cloud core (e.g., Pringle 1989) and growth of an instability in the outer parts of a massive circumstellar disk (e.g., Bonnell 1994). In the first case, if we neglect long term tidal interactions, fragmentation could yield non co-planar systems, if the initial cloud is elongated and the rotation axis oriented arbitrarily with respect to the cloud axis (see Bonnell et al. 1992). In the second case the disks around both binary components will always be co-planar, thus the stellar spin axes aligned.

The respective orientation of the system components' rotation axes therefore appears as an important geometrical parameter of a forming multiple system to disentangle between the various formation models. Unfortunately, such a determi-

Send offprint requests to: J.-L. Monin, (Jean-Louis.Monin@obs.ujf-grenoble.fr)

⋆ Based on observations made with the Bernard-Lyot Telescope at the Pic-du-Midi observatory and with the Canada–France–Hawaii Telescope, operated by the National Research Council of Canada, the Centre National de la Recherche Scientifique de France and the University of Hawaii.

nation is currently poorly constrained by observations. Our understanding of the stellar formation will be greatly improved when we establish the respective repartition of the axes orientations. Previous studies of the projected rotational velocities of both components of visual binaries on the main sequence by Weis (1974) and Hale (1994) showed a directional correlation of orbital and rotational axes, indicating a tendency toward spin alignment for systems with separation less than 30-40 AU. Within the framework of star formation theory, this distance is smaller than the size of an accretion disk, leading to think that star-disk interactions are indeed important in determining the final system structure. However, these studies concern stars on the main sequence where all the star-disk and disk-disk interaction processes between the components are likely to have ceased and the state of the system do not reflect the initial binary formation conditions anymore.

In PMS binary systems, the projection of the rotation axes of both components on the line-of-sight can be obtained through the combination of the projected rotational velocity, $v \sin i$, the rotational period, and an estimate of the stellar radius. This determination is quite indirect and can induce large uncertainties. In this paper, we propose to use linear polarization measurements to determine the other angle that defines the three-dimensional orientation: the projection of the rotation axis in the plane of the sky. The basic idea relies on the fact that in T Tauri stars, linear polarization in the visible range is caused mostly by scattering. As a consequence, it retains information about the geometry of the circumstellar environment of each component, allowing evaluation of the symmetry axis of these environments. We have started a study of the linear polarization of individual components in PMS binaries in nearby star formation regions, including Taurus-Auriga.

Sect. 2 presents a description of our method, together with the expected limitations resulting from the finite signal-to-noise ratio. A review of polarimetric measurements on wide binaries ($> 8''$) in the literature is presented in Sect. 3, together with a test of the method on closer binaries ($< 6''$, all but one being $< 3''.2$), for which we have also observed individual spectra in order to assess their nature, classical or weak-line TTS (resp. CTTS or WTTS). The results are presented in Sect. 4 and discussed in Sect. 5. Expected improvements in the near future and a conclusion are given in Sect. 5 and Sect. 6.

2. The method

2.1. Description

The main idea behind the method is that if both components in a binary have an axisymmetric circumstellar medium and have a detectable polarization, then this polarization reliably traces the orientation of the symmetry axis of their circumstellar environments, and therefore their rotation axes. In order to get a sufficiently large intrinsic polarization, both components must be surrounded by a sufficient amount of dust and gas, and the inclination with respect to the line-of-sight must be large enough. Our method is thus likely to give good results when applied to binaries where both components are CTTS.

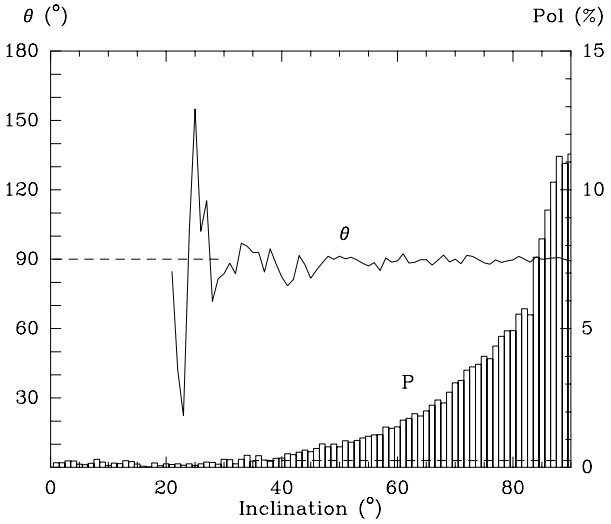

Fig. 1. Polarization Model. The polarization level P (histogram) and its position angle θ (solid line) are computed for a bipolar nebula surrounding a circumstellar disk. The position angle is not well defined for P$< 3\sigma(P)$, i.e., below 40° when $\sigma(P) = 0.1\%$ (the horizontal dashed line at the bottom of the polarization histogram corresponds to P=0.3%; it intersects the polarization histogram at an inclination $\approx 40°$). The position angles below 20° are not shown.

Models of bipolar reflection nebulae by Bastien and Ménard (1990) have shown that the position angle of the integrated linear polarization of the scattered starlight is parallel to the equatorial plane of the disk, provided the inclination is sufficiently large. Indeed if the star is seen at low inclination, say less than $30°$, the integrated polarization level will decrease toward $P = 0$, a value reached if the system is seen face-on. On the other hand, for larger values of the inclination and assuming all CTTS are associated with small, unresolved, bipolar nebulae, one can estimate the projected orientation of the symmetry or rotation axis of the system by measuring the position angle of the linear polarization vector.

Our calculations assume that the star+disk system is surrounded by a large bipolar dust enveloppe scattering a fraction of the photons received by the observer, and making the polarization position angle appear parallel to the equatorial plane. Fig. 1 shows the resulting polarization level P and position angle θ computed for a bipolar reflection nebula with a multiple scattering code (Ménard 1989). We use the density structure given by Galli & Shu (1993), for the $\tau = 0.7$ case (see their Table 5 and Fig. 1c). The reflection nebula has a radius of 3000 AU ($20''$ in Taurus), and an accretion disk was added to that prescription, the disk being defined as an abrupt density increase by a factor of 20, over a radius R=250 AU and a "flaring" angle of $5°$. The results show that if one can reach a polarization uncertainty σ(P) of $0.1\,\%$ or better, the position angle of the polarization is well defined and parallel to the disk (PA=90^o) for all inclinations larger than 40^o. Therefore, this method gives a reliable estimate of the disk orientation for inclination angles larger than approximately 40^o.

If no envelope is present, the received photons will be scattered by the disk and this different scattering geometry results in a integrated polarization perpendicular to the disk plane instead. Whitney & Hartmann (1992) and more recently Wood et al. (1998) have modeled such situations, and their results show that in all cases, for a large enough inclination, the polarization is perpendicular to the disk plane rather than parallel to it. However, this 90^o shift on the position angles of the polarization in the models does not impede our ability to estimate the orientation of T Tauri stars. Two T Tauri stars having different orientations within a binary system will have different polarization position angles, whether or not a dust envelope is dominant. In the following, we assume that all the CTTS of our sample are associated with small, unresolved, bipolar nebulae with a dusty envelope surrounding their accretion disk, and that the polarization measurement integrates the whole star+disk+envelope system.

Note that the measured polarization level cannot be used, in conjunction with Fig. 1, to evaluate the inclination angle directly. The integrated polarization levels are sensitive to the exact density distribution: the total extinction on the line-of-sight, the radial dependence of the density profile, the grain size and type, so that Fig. 1 is valid only for one given model. Note also that the exact value of the inclination angle for which $P > 3\sigma(P)$ ie. $\sigma(\theta) < 10°$, is model dependent. Nevertheless, two features appear general and useful to derive the orientation of stars in binary systems: 1) the integrated polarization level rises when the inclination increases, 2) within our hypotheses, the integrated polarization position angle remains parallel to the disk plane whenever the polarization is large enough for the angle to be well defined. It is this latter result that we will use to assert the projected orientation in the plane of the sky of the CTTS of our sample for which a significant polarization is detected.

2.2. Linear polarization imaging

The polarization measurements obtained with classical photoelectric polarimeters are limited to binary separations of a few arcsecs because of the diaphragm sizes used, typically 3-4″ or more. We have tested the method proposed in Sect. 2.1 on closer binaries by using imaging linear polarimetry instead. The seeing is then the limiting factor to resolve binaries. In practice it allows a study of tighter systems than classical aperture polarimetry does.

In imaging polarimetry, one way to measure the polarization is to obtain 3 images through linear polarizers oriented differently, say at 0^o, 60^o and 120^o from the north celestial pole. Each image yields a measure of the polarized intensities I_0, I_{60} and I_{120} for each component of the binary. This polarimeter is very easy to implement on any imaging camera. Instrumental polarization can be limited to a minimum by installing the polarimeter at the Cassegrain focus and by rotating the whole instrument instead of the polarizers only. The details of the computations to transform I_0, I_{60} and I_{120} into P and θ are given in Appendix A.

Table 1. Numerical simulation results; see text for details.

S/N		model			calculated polarization	
		prim.	sec.	ref.	prim.	sec.
150	P	1	1	0	1.1 (1.2)	1.1 (1.4)
	θ	25	55		24 (32)	54 (32)
240	P	1	1	0	1.0 (0.8)	1.0 (0.9)
	θ	25	55		25 (22)	56 (20)
400	P	1	1	0	1.0 (0.4)	1.0 (0.4)
	θ	25	55		25 (9)	54 (9)
580	P	1	1	0	1.0 (0.3)	1.0 (0.3)
	θ	25	55		24 (8)	56 (7)

This formalism assumes that the only variations between the subsequent frames at 0^o, 60^o and 120^o come from polarization effects and not from sky transparency fluctuations (i.e., observations are made in perfect photometric conditions). This puts a strong constraint on the method as we will see; it limits its ability to measure low polarizations.

To avoid this limitation, one can use the fact that one or many field stars can also be detected on the images. By assuming these stars to be unpolarized, because for example they are foreground stars, one can monitor and compensate the photometric variations between each exposure. Unfortunately, T Tauri stars are found in molecular clouds and nearby unpolarized field stars are quite rare, and often too faint for accurate photometry, making this photometric monitoring method difficult most of the time.

Limits on these affirmations can be given by numerical simulations. To estimate the signal-to-noise ratio needed on the field star in each individual image to reach accurate polarimetry, we built artificial images similar to the ones observed (i.e., same separation between stars, same FWHM, same readout noise...). We considered a bright primary, a fainter secondary, and a much fainter reference star. The primary and the secondary are polarized, the field star is not. The results are presented in Table 1. Column 1 gives the signal-to-noise ratio at which the field star used as a photometric reference is detected. In all cases, the primary T Tauri star has SNR=1900, and the secondary has SNR=1250. Columns 3, 4, and 5 give the polarization characteristics of the primary, the secondary and the reference star respectively. The top line gives the polarization level P, the bottom line gives the position angle θ. The polarization level on the primary and the secondary are set identical while the angles differ by 30^o. Columns 6 and 7 give the calculated polarization, with the errors in parenthesis, of the primary and secondary assuming the faint reference field star is unpolarized. The formalism of Appendix A is used.

The results presented in Table 1 show that in order to get an absolute precision better than 0.3% on the linear polarization level, photometric measurements with S/N ≥ 580 are needed on each individual image of the reference star if it is truly unpolarized. This would be valid for example for a CTTS binary located inside a molecular cloud and a reference star located

well in front of it and not suffering from interstellar polarization.

Reference stars effectively unpolarized are hard to find in practice, as the stars detected in the same frames as the target will most likely be affected by interstellar polarization. Further simulations were thus performed to estimate the effect of a reference star with a non-zero polarization. This would be expected for example for a reference star located also within the molecular cloud and suffering from the same interstellar polarization as the binary. In that case, if we assume the reference star to be unpolarized while its actual polarization is similar to that of the binary, the polarization of the primary and secondary cannot be recovered. This is true even if the S/N is larger than 580. The use of a reference star with a known and constant polarization is also possible. However, in practice we do not expect to find many of them in the same field than our sources, and this requires more than excellent photometric conditions.

To summarize, a S/N = 580 or more is necessary to measure the polarization of a star with a $1\,\sigma$ accuracy of 0.3% on P, the polarization level. This is valid only if the reference star used to monitor the sky transparency is unpolarized, or if the sky is perfectly photometric if no on-frame reference star is used. The impact of non-photometric conditions will be discussed in Sect. 4.3.

3. Observations and data reduction

3.1. The sample

Our sample is divided into two sets. A large separation set has been obtained from the literature and concerns binaries with separations larger than $8''$. The second set is made of closer binaries, with separations less than $6''$, most of them being closer than $3.2''$.

To construct the large separation set we surveyed the literature, looking for binaries for which polarimetric data are available for each individual component. The lower limit on the separation ($8''$ or ≈ 1120 AU at the distance of Taurus) is such that no contamination occurs from the other component, while the upper limit set at $\sim 35''$ (≈ 5000 AU) ensures that there is little contamination by (unbound) visual pairs.

We have selected only measurements taken with the same instrument through the same filters and at the same time for a given binary. This is important to avoid contamination by likely intrinsic polarization variations, which are quite common for TTS (Ménard & Bastien, 1992). Such variations affect P and θ, and most of the time, the polarization vector wanders back and forth about a given value with a limited amplitude. In the following, we will assume that the values presented in this paper are representative of an average position angle of the polarization. This large separation subsample of binaries is presented in Table 2.

The second data set contains binaries with separation less than $3\farcs2$, except for one at $5\farcs9$, and have been chosen from a list published by Mathieu (1994). Stars were selected because of their large excess flux ratio over a photosphere at $10\,\mu$m ($\Delta N > 1.1$, see Skrutskie et al., 1990) and/or their high flux at $12\,\mu$m (IRAS) and 1.3 mm, suggesting their CTTS nature and indicating the presence of a large amount of circumstellar material, likely in the form of a disk. Table 3 presents the main characteristics of this subsample. The data given in this table were taken in Mathieu (1994) and references therein.

Table 2. The sample of wide TTS binaries (sep. $> 8''$). The HBC numbers of the (brighter in V) primaries are boldfaced.

Object	HBC	sep.($''$)	PA ($^\circ$)
035120+3154 SW/NE	**352**/353	8.7	71
040047+2603 W/E	358/**359**	23.5	22
V773/FM Tau	**367**/23	37.3	13
DI/DH Tau	**39**/38	15.0	306
FY/FZ Tau	401/**402**	16.9	71
V807/GH Tau	**404**/55	21.5	195
GI/GK Tau	**56**/57	12.9	328
HP Tau /G2 /G3	66/**415**/414	20.9 / 9.7	297 / 244

Table 3. The sample of close TTS binaries (sep. $< 6''$) with HBC number of the primaries boldfaced when available.

Object	HBC	Sep. ($''$)	P.A. ($^\circ$)	ΔN	$F_{12\mu}$ (Jy)	$F_{1.3mm}$ (mJy)
UX Tau AB	**43**/42	5.9	269	1.31(A)	0.30	73
UX Tau AC	**43**	2.7	181	1.31	0.30	73
DK Tau	45	2.5	115	1.93	2.24	35
HK Tau	48	2.4	175	1.47	0.31	41
V710 Tau	**51**/395	3.2	357	1.15	0.35	71
HN Tau	60	3.1	215		1.59	<45
Haro 6-37	**73**/424	2.7	37	1.75	1.20	60

The triple system of UX Tau has been treated as 2 separate binaries with the same primary HBC 43.

3.2. Spectroscopy

We have obtained spectrometric measurements of the close binaries listed in Table 3 (to the exception of V 710 Tau), in order to evaluate the spectral type of each star, assess their nature as CTTS or WTTS, and study the pairing statistics. The observations were performed during the nights of 1995 december 27 & 28 at the Canada-France-Hawaii 3.60m telescope. The Stabilized Image Spectrometer (SIS) was used with a 2048×2048 CCD. The plate scale was $0\farcs17$ per pixel. The starlight was dispersed from 4000 to 8000 Å using a grism, with a final resolution of 3.7 Å/pixel. DK Tau has been measured during the first night with a $0\farcs7$ slit under subarcsecond seeing. All other sources were measured during the second night with a $1''$ slit under $1\farcs2$ seeing. Observations of the calibration stars Feige 25 and Feige 56 were performed every night. The integration time was 300 s in all cases except for DK Tau (500 s).

Data reduction was performed with the *Longslit* and *Onedspec* spectra reduction packages of NOAO/IRAF. The spectra

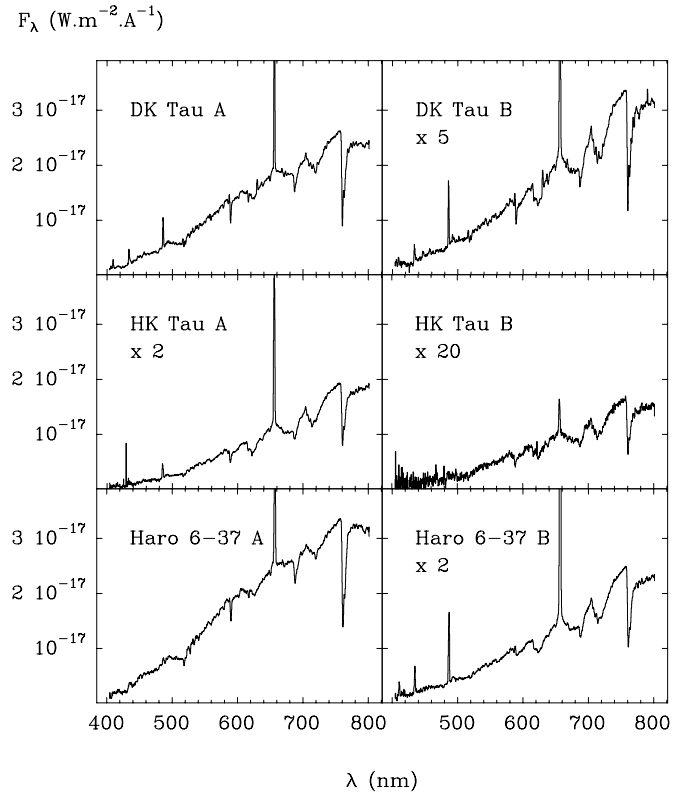

Fig. 2. Spectra of the sources with similar spectral types. The intensity range has been fixed (units in W.m^{-2}.Å^{-1}), and some of the spectra have been scaled so that the spectral features are clearly visible. The wavelength units are expressed in nm.

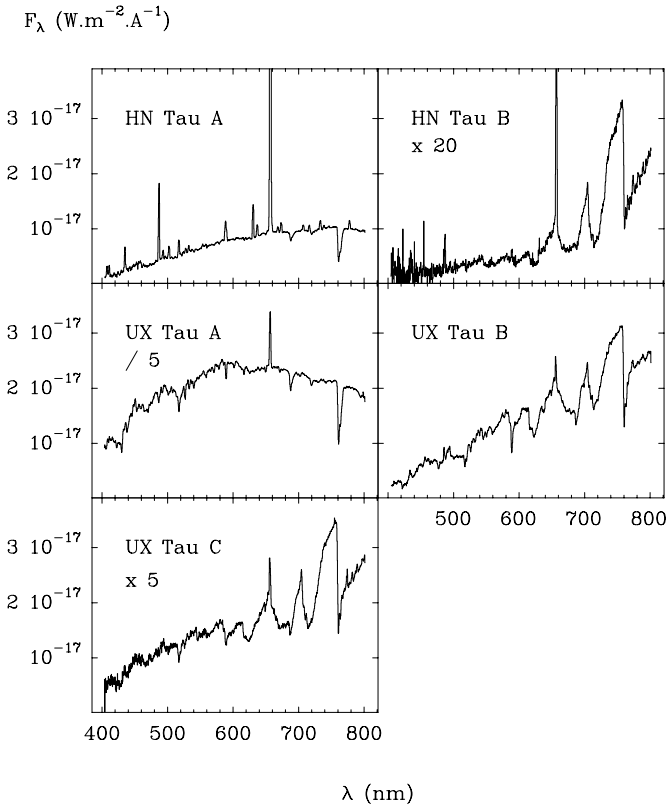

Fig. 3. Same as in Fig. 2 for HK Tau and UX Tau

have been corrected for transmission variations using the spectra of Feige 25 and Feige 56. In order to extract the spectrum of each component of the closer binaries, we have fitted two gaussian profiles on every line of the CCD, under the constraint that the width of each gaussian (selected to match the seeing value) must be the same for both components. The results of this extraction procedure are presented in Figs. 2 and 3.

3.3. Imaging polarimetry

In order to test the method on tighter binaries, we have obtained polarimetric images in the I-band for each star in Table 3, during the night of 1995 November 19, at the 2m Bernard-Lyot Telescope (TBL) of the Pic-du-Midi observatory. An additionnal star, V710 Tau, was also imaged. The camera used at the f/25 Cassegrain focus was equipped with a 1024×1024 TEK CCD. The readout noise was ≈ 16 electrons. The focal plate scale was $0\farcs2$ per pixel (square field-of-view of $3\farcm4$ per image). The seeing (FWHM as measured on the reduced images) was $\sim 0\farcs8$, stable over the night. Two filters were used. A plain I-band filter for direct imaging and an I + polaroid sheet sandwich for polarimetric imaging. Three images at 3 different position angles ($0°$, $60°$ and $120°$) were obtained for polarimetry by rotating the complete filter+camera assembly. This procedure minimizes the intrumental polarization contamination. The instrumental observing conditions were therefore constant over the 3 images. Each binary was observed twice with a given polarization position angle in order to remove the cosmic rays and increase the S/N ratio without saturation. Flat fields were taken for each position angle of the polaroids against the sun-rising sky.

After correcting for bias, flat field and cosmic rays, the photometry of every star in the field for every position of the polaroids was done with the IRAF *Daophot* package. Then the P and θ parameters were determined for every binary component, using the formulae given in Appendix A.

4. Results

4.1. Spectroscopy

The spectra of the 5 sources observed are presented in Figs. 2 and 3 (see captions for details). In every source, the primary (defined as the brightest component in V) is referred to as A, and the secondary as B. Out of the 5 pairs, 3 show similar spectral types for both components: DK Tau, HK Tau and Haro 6-37 (see Fig. 2). In HN Tau and UX Tau, the primary appears significantly hotter than the secondary (see Fig. 3).

For detected emission lines, the equivalent widths are given in Table 4, together with the spectral types and the corresponding effective temperature, from Cohen & Kuhi (1979). Errors on the equivalent widths are typically 5%, except for the [OI]λ6300 Å line in HN Tau B, where it reaches 30%. Errors on the spectral

Table 5. Polarization data for the wide binaries. The results are listed two by two in the same order as in Table 2 (to the exception of the triple star HP/G2/G3) with the primary component listed first. Moneti et al. (1984) did not provide uncertainties for their V807/GH Tau polarization measurements.

Object	P (σ_P) (%)	θ (σ_θ) (°)	λ Å
035120+3154 SW	1.42 (0.1)	60 (2)	7675
035120+3154 NE	0.93 (0.1)	58 (3)	7675
040047+2603 E	0.25 (0.1)	115 (10)	7675
040047+2603 W	0.3 (0.1)	93 (10)	7675
V773 Tau	0.28 (0.1)	77 (10)	K†
FM Tau	1.66 (0.8)	105 (13)	K†
DI Tau	0.4 (0.1)	151 (7)	7675
DH Tau	0.05 (0.1)	—	7675
FZ Tau	1.6 (0.16)	80 (3)	7675
FY Tau	2.16 (0.15)	78 (2)	7675
V807 Tau	0.9	52	J†
GH Tau	0.8	60	J†
GI Tau	0.73 (0.12)	117 (5)	7675
GK Tau	1.25 (0.12)	42 (3)	7675
HP Tau	2.65 (0.14)	63 (2)	7675
HP Tau /G3	2 (0.2)	69 (3)	7675
HP Tau /G2	2.4 (0.12)	73 (2)	7675

† J= 1.25μm, K= 2.2μm

types are 0.5 subclass for types later than M0, and 1 subclass for the others. They translate into errors of 0.01–0.02 dex on log($T_{\rm eff}$), from M to mid-K, to which 0.02 dex should be added due to a systematic overestimate caused by the choice of luminosity class (IV for PMS stars, instead of V tabulated by Cohen & Kuhi).

4.2. Polarimetry of the wide binaries

The polarization data were collected from the literature. They are reported in Table 5. The data are from Tamura & Sato (1989) for V773/FM Tau, from Moneti et al. (1984) for V807/GH Tau, and from Ménard et al. (1998) for all others. We have quoted the value of the polarization level P for each component of the binary, together with the uncertainty $\sigma(P)$. When the ratio $P/\sigma(P)$ was larger than 3, we have also quoted the polarization position angle θ and its uncertainty $\sigma(\theta) = 28.6° \times \sigma(P)/P$.

The separations range between $8\farcs7$ and $37\farcs3$, or 1200 AU and 5200 AU, assuming a distance of 140pc for Taurus. We consider the HP Tau group as two binaries, HP Tau/HP Tau G2 and HP Tau G3/HP Tau G2. The separations are given in that order in Table 2.

The goal of this section is to check whether the orientations of wide binary components are similar or not. Two conditions are necessary: the polarization must be detected, and it must be intrinsic to the objects, i.e., not of interstellar origin. We argued in Sect. 2.1 that CTTS/CTTS pairs, viewed with a large inclination are the best candidates for that study.

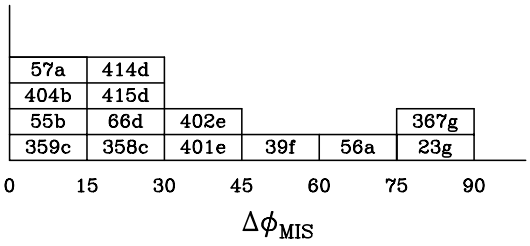

Fig. 4. Histogram of the difference $\Delta\phi_{MIS}$ (in degrees), between the position angles of the polarization measured on star and the local interstellar polarization. The binaries are labeled by they primary HBC number (see Table 2) together with a supplementary letter (a-g) used to match each pair / group.

If the polarization were of interstellar origin, both components would appear with parallel polarizations because in clouds like Taurus, the interstellar polarization changes on scales much larger than the separations considered here. A few other clouds however, might have more than one polarization component with different interstellar polarization position angle for a given line-of-sight. This may lead to difficulties in evaluating the interstellar polarization. This is not the case for our data in Taurus. We have used the data of Goodman *et al.* (1990) and Tamura & Sato (1989) to evaluate the position angle of the interstellar polarization at the location of the wide binaries and compare it to the stars' polarization position angle. The results are presented in Fig. 4 and show a smooth correlation, with many objects having a measured polarization similar to the interstellar one to better than $30°$. Among these objects, many are part of the same pair, indicating that the interstellar medium plays a role, at least partly, in this apparent alignment.

Fig. 5-a presents the results of a search for a correlation between the polarization position angles of each component. The positive result $\Delta\phi_{BC} < 30°$ in all cases but one, suggests that the stellar symmetry axes are mostly parallel in the binaries we considered. In the following, we check each individual result against the interstellar contamination.

The CTTS binary V807 Tau/GH Tau (HBC **404**/55) appears in the $0-15°$ bins of both Fig. 5-a and Fig. 4 and its polarization is low. We conclude that this apparent correlation is dominated by interstellar polarization. This is also the case for the WTTS binary HBC 358/**359**, as expected for WTTS stars. Although we cannot check the interstellar polarization very close to the other WTTS binary of the sample HBC **352**/353, we believe its apparent parallel orientation is also dominated by interstellar polarization.

The HP Tau group (HBC 66/**415**/414) contains stars that are highly polarized but show only a moderate $15° - 30°$ polarization position angle difference with the local interstellar value. Moreover, the two companions (G2 and G3) are WTTS stars. This group is probably affected by interstellar polarization, although it is at the upper end of the values measured in Taurus.

The pair FY/FZ Tau (HBC 401/**402**, both CTTS) is highly polarized at angles similar for both objects but otherwise very different from the interstellar polarization value. Similarly, the

Table 4. TTS type, equivalent widths in Å of detected emission lines, spectral types and $\log(T_{\rm eff})$ for stars of the small separation subsample.

Object	TTS type	H_α	H_β	H_γ	H_δ	He I 6678Å	[OI] 6300Å	[OI] 6363Å	[SII] 4069Å	[SII] 6717-31Å	Spectral Type	$\log(T_{\rm eff})$
UX Tau A	w	9.5									K4	3.661
UX Tau B	w	4.5	3.5	3	2						M2	3.544
UX Tau C	w	8.5									M3	3.526
DK Tau A	c	31	16	24	16	0.7	2.4	0.5	4.5	0.6	K9	3.598
DK Tau B	c	118	33.5	19	11.5	1.5	4.5	1.5	11		M1	3.566
HK Tau A	c	50	20	18							M1	3.566
HK Tau B	c	12.5									M2	3.544
HN Tau A	c	230	64	23	17.5	2.5	16.5	7	22	5	?e	
HN Tau B	c	65	41	47		2	6				M4.5	3.502
Haro 6-37 A	c	19.5	3.7	7.5							K8	3.598
Haro 6-37 B	c	195	60	38	26						M0	3.593

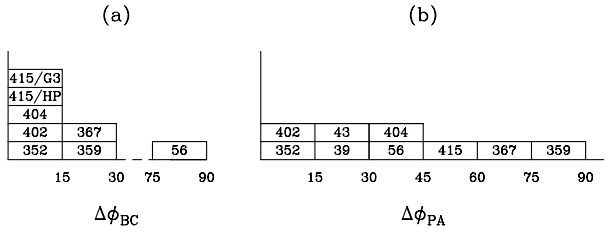

Fig. 5. a Histogram of the differences $\Delta\phi_{BC}$ (in degrees) between the polarization position angles of the binary components in the wide binary sample (left). There is no object in the 30-75° range. **b** Histogram of the difference $\Delta\phi_{PA}$ between the *primary* polarization position angle and the binary position angle (right). In both histograms, binaries are labeled by their primary HBC number as in Fig. 4 to the exception of HP Tau which is a triple system.

CTTS pair GI/GK Tau (HBC **56**/57) exhibits polarization position angles that are very different for both components, ruling out an interstellar origin, at least for GI Tau.

V773/FM Tau, (HBC **367**/23) have parallel polarizations within the error bars. This orientation is perpendicular to the local interstellar value. This object is peculiar because the only published simultaneous polarization measurements were obtained in the infrared, at $2.2\,\mu$m. The 90° difference is not an optical depth effect (because of the longer wavelength) because polarization position angles measured in the optical are similar. However, the polarization position angle of V773 Tau is extremely variable (Ménard and Bastien, 1992). It rules out an interstellar origin but makes it difficult to assess the orientation reliably. We have used the simultaneous $2.2\,\mu$m results in our histograms of Figs. 5 and 4.

Finally, we also searched for a link between the polarization position angle of each member and the apparent position angle of the binary, (Fig. 5-b). No correlation is found between the primary's polarization position angle and the apparent binary position angle. It suggests that the polarization is probably not circumbinary in origin. However, the lack of a correlation does not mean that the disks are not coplanar with the orbital plane. In particular, the position angle of the binary may not necessary be aligned with the position angle of a possible circumbinary envelope.

4.3. Polarimetric imaging on close binaries

The results show that HN Tau A is significantly polarized: 2.7% +/- 0.4%. This is in agreement with measurements by Ménard et al. (1998) and Tamura & Sato (1989). DK Tau B is also marginally detected.

However, no significant detection of the polarization was made on any other object. This appears surprising in view of our simulations in Sect. 2.1 and the large S/N ratios effectively reached in the observations. The S/N for the primaries were $1310 \leq (S/N)_{\rm prim} \leq 3045$, they were $640 \leq (S/N)_{\rm sec} \leq 1270$ for the secondaries. We would have expected reliable estimates of the polarizations from these numbers. However, the S/N reached for the reference stars are below the criterion given in Sect. 2.2 ($80 \leq S/N_{\rm ref} \leq 405$). For such reference star S/N values, our simulations in Table 1 show that the polarization is hardly measured with a precision better than $2\,\sigma$.

Moreover, these results raise questions regarding the ability of rotating polaroid sheet/wire grid imaging polarimeters to perform high accuracy polarimetry. We suspect non-photometric conditions to be partly responsible for the large error bars and the lack of detections, as a $1\,\%$ photometric error on one of the 3 frames at $0°$, $60°$ and $120°$ translates into a slightly larger polarization error on P. From the photometry point of view, this is not a large error, but from the polarimetry point of view, this is a large error. Suggestions for improvement will be presented in Sect. 5.2.

Since we are interested in the *relative* orientation of the components, we can go further and try to calculate relative polarizations, which are easier to measure precisely. We have applied the same direct method to compute the *relative* polarization of the secondary in every pair, using the high S/N primary as a reference, and arbitrarily setting its polarization to zero. The corresponding results are presented in Table 6 and should be interpreted as follows. When significant relative polarization is

Table 6. Polarizations of the secondary component relative to the primary for the close binary sample.

Object	rel. P (%)	(σ_P) (%)
UX Tau AB	1.11	0.59
UX Tau AC	2.39	1.20
DK Tau	2.90	1.43
HK Tau	2.72	1.93
V710 Tau	0.16	0.38
HN Tau	3.27	1.09
Haro 6-37	0.80	0.44

"detected", it means that the polarization of the secondary is different than the primary's, either in level, or in angle.

Although the S/N ratio is better, it still falls short of the accuracy we should have reached. HN Tau remains the only system where the polarizations of the two components are clearly different. In all other cases, the relative "detection" of the secondary against the primary is not significant at a $2\,\sigma$ level.

5. Discussion

5.1. Physical considerations

For objects without dominant interstellar contamination, one of the results of this paper is that at least on one occasion, for GI Tau/GK Tau, the components' axes are *not* parallel. On the other hand, we find that 2 other wide binaries show polarization vectors of their components that are aligned: FY Tau/FZ Tau, V773 Tau/FM Tau. There is another pair, DI Tau/DH Tau for which we lack information on the secondary but where the primary most likely has an intrinsic polarization. The relative orientations discussed above are projections in the plane of the sky. The other angle needed to have the complete 3-dimensional orientation, the inclination i, is available only for a very limited number of sources. We have used rotation data from Bouvier et al. (1986), Hartmann et al. (1986) and Vrba et al. (1989) to compute this parameter. However, measuring the stellar luminosity of a PMS star is a difficult challenge, and subsequent computations leading to the $\sin i$ value can induce even more uncertainties. If we use the recent stellar data from Kenyon and Hartmann (1995), we find that GI Tau and GK Tau have inclinations of $i = 73°$ and $i = 48°$ respectively. These values could even be considered compatible (say $60° \pm 10°$), given the uncertainties. However, these two stars have very different polarization position angles, suggesting that rotation axes are not parallel in space. We also find that HP Tau and HP Tau/G2 have similar inclination angles. Since their polarizations are parallel it is tempting to conclude that these stars have indeed parallel rotation axes. However, their polarization is likely contaminated by interstellar (or intracluster) polarizations. Careful observations at many wavelengths would help extract the intrinsic part of the polarization and provide confirmation for this finding.

It is difficult to compare our results with those obtained for main sequence stars by Weis (1974) and Hale (1994). Two out of the four pre-main sequence pairs for which the polarization method is applicable have parallel axes. We cannot draw conclusions, but we note that these PMS and MS distributions are compatible, with the warning that strictly speaking, we do not have access to the coplanarity information for our PMS stars, since the orbital elements are unknown.

Concerning the binaries found with parallel axes at large separations, we favour the hypothesis that this orientation reflects their initial formation conditions, rather than resulting from evolutionary effects. On the other hand, we also find that there exist at least one system where the components' axes are *not* parallel. This is a very exciting result, as most of the current fragmentation models predict parallel axes if not coplanar systems (e.g., Bonnell et al. 1992).

Of interest are also our results on the respective determination of the spectra of both components in our close PMS binaries sample. If we distinguish between CTTS and WTTS according to whether their H_α equivalent width is more or less than 10 Å (see Table 4), we find that if one of the binary component is a classical TTS, so is the other when the separation is small. There is no mixed pair (CTTS+WTTS) in our close binary sample, to the possible exception of UX Tau where the primary can be classified as a CTTS according to its H_α flux. These results confirm the trend already observed by Prato and Simon (1997). On the other hand, not every primary is the more active component, i.e., presents the larger H_α flux. In Haro 6-37 for instance, the primary is approximately 3 times brighter than the secondary and the latter has a 10 times larger H_α equivalent width than the former so that its H_α flux is more than 3 times larger.

The approach we proposed here to get insights into the process of star formation and the geometry of the collapse seems promising in view of our preliminary results. Hopefully, campaigns to study larger samples will be carried out in the near future.

5.2. Technical considerations

The scope of our study on close binaries was limited by our inability to obtain high accuracy polarimetry with a simple optical polaroid-sheet imaging polarimeter. With this class of polarimeters, we showed that high S/N ratio images are not sufficient to reach an accuracy limited by photon noise and therefore to guarantee high accuracy polarimetry. From a sample of 122 stars, Ménard & Bastien (1992) calculated an average optical integrated polarization of $\sim 1.7\%$ for T Tauri stars located over the whole sky. In Taurus, the average is 1.6% for CTTS and 0.7% for WTTS (Ménard et al. 1998). Current single beam polarimetric imagers provide σ_P of the order of $0.5 - 1\,\%$; this is unsufficient and more accurate instruments are needed to study the bulk of this binary sample.

The dominant limiting factors are the photometric fluctuations (i.e., atmospheric transparency fluctuations, and to a lesser extent seeing variations) of the atmosphere on short time scales, between each exposures. These variations lead to different inten-

sities that propagate into large polarizations and/or large errors on the measurements. In practice, because of the atmosphere, errors on the polarization σ(P)$< 1\%$ are difficult to achieve without extra careful monitoring of the atmospheric transparency. Furthermore, the photometric data reduction process itself limits the accuracy to σ(P)$\sim 1\%$ in the optical, mainly because of limitations on (polarization dependent) flat field accuracies and of the error propagation in the combination of the many different exposures needed to extract the polarization. This number should be increased when an infrared detector is used.

Better polarimetric accuracies could be obtained with dual-beam polarimeters measuring the intensities in two orthogonal directions simultaneously. Then the two beams are affected by the same atmospheric fluctuations and the measured normalized Stokes parameter, given by $(I_{\parallel} - I_{\perp}) / (I_{\parallel} + I_{\perp})$, is free from photometric variations, yielding higher accuracies under most observing conditions. Accuracies σ(P)$\leq 0.5\%$ should routinely be achieved.

6. Conclusion

We described a method to use polarimetric measurements to get information on the alignment of the rotation axes of both components of PMS binaries. It gives the projection in the plane of the sky of the symmetry axis of bipolar nebulae. We argued that this method is efficient for classical T Tauri stars seen at a large inclination angle.

This information complements the measure of the inclination angle on the line-of-sight resulting from $v \sin i$ measurements. We have surveyed the literature for measurements on binaries with separation larger than the seeing, and we used polarimetric imaging, with a simple linear polarizer and a CCD to check for the respective polarization in close binaries. Numerical simulations and careful study of our data show that this method is heavily dependent on the atmospheric conditions, and to a lesser extent on the interstellar polarization. However, qualitative results are found for a few objects.

First results on four wide (< 5000 AU) PMS low-mass binaries in Taurus suggest that alignement of the symmetry axes occurs at a rate compatible with that measured on the main-sequence. Because it concerns wide binaries, this alignment is thought to result from initial binary formation itself rather than via a posteriori tidal interactions. The method is promising but requires the use of more accurate polarimeters. We demonstrated that in most cases, single-beam polarimeters with polaroid-sheet (in the optical) or wire-grids (in the near-infrared) are inadequate.

To confirm the nature of the binary members, visible spectroscopy was performed. It allowed us to determine accurate spectral types along with Balmer and forbidden lines equivalent widths. Our measures confirm previous results that binaries are not randomly paired. We also find that in some cases the secondary component can have a larger H_α flux than the brighter primary. We will present in a forthcoming paper (Duchêne et al. 1998), an extensive study of the respective accretion activities of both components in tight binaries.

The next step in this disk orientation study would consist of using a high angular resolution device and a polarimeter, to get the same information for closer binaries, where different formation mechanisms may be considered and tidal interaction get more important. From the spectrometric point of view, it will be interesting, in those close binaries, to search for a correlation between primary's and secondary's accretion or mass-loss as a function of the separation, indicating how the presence of a companion tends to influence the disk accretion at small distances.

Acknowledgements. We thank the TBL staff for its help during the linear polarimetric images observations and Ch. Vanderriest for the remote observing of the spectra at the CFHT. We thank J. Bouvier for providing us with an IRAF routine to extract the individual spectra of the binary systems. This research has made use of the Simbad database, operated at CDS, Strasbourg, France, and of the NASA's Astrophysics Data System Abstract Service.

Appendix A: polarization computations

The polarization level P together with the position angle θ of the polarization vector are obtained through 3 measurements through linear polaroids, at 3 different angles : 0°, 60° and 120°. From the 3 corresponding intensities I_0, I_{60}, and I_{120}, we deduce the Stokes parameters I, U and Q, together with their uncertainty :

$$
\begin{aligned}
I_{tot} &= \frac{2}{3}(I_0 + I_{60} + I_{120}) \\
\sigma_{I_{tot}} &= \frac{2}{3}\sqrt{(\sigma_{I_0})^2 + (\sigma_{I_{60}})^2 + (\sigma_{I_{120}})^2} \\
Q &= \frac{4}{3}I_0 - \frac{2}{3}(I_{60} + I_{120})) \\
\sigma_Q &= \sqrt{\frac{16}{9}(\sigma_{I_0})^2 + \frac{4}{9}((\sigma_{I_{60}})^2 + (\sigma_{I_{120}})^2)} \\
U &= \sqrt{\frac{4}{3}}(I_{60} - I_{120}) \\
\sigma_U &= \sqrt{\frac{4}{3}((\sigma_{I_{60}})^2 + (\sigma_{I_{120}})^2)}
\end{aligned}
$$

and we compute the degree of polarization P and the position angle θ and their uncertainty from:

$$
\begin{aligned}
P &= \frac{\sqrt{Q^2 + U^2}}{I_{tot}} \\
\sigma_P &= P\sqrt{(\frac{\sigma_{I_{tot}}}{I_{tot}})^2 + \frac{(Q\sigma_Q)^2 + (U\sigma_U)^2}{(Q^2 + U^2)^2}} \\
\theta &= \frac{1}{2}\arctan\frac{U}{Q} \\
\sigma_\theta &= \frac{1}{2}\frac{\sqrt{(U\sigma_Q)^2 + (Q\sigma_U)^2}}{U^2 + Q^2}
\end{aligned}
$$

Note that an equivalent form of these equations was first used by Redman et al. (1986). Also, the equations given here

(including the errors) were derived by Asselin (1991) and used (but not given) by Asselin et al. (1996). We give them all here for completeness and future reference.

References

Asselin, L., 1991, M. Sc. Thesis, University of Montréal.
Asselin, L., Ménard, F., Bastien, P., Monin, J.-L., and Rouan, D., 1996, ApJ, 472, 349
Bachiller, R. 1996, ARA&A, 34, 111
Bastien, P. & Ménard, F. 1990, ApJ, 364, 232
Bonnell, I.A. 1994, MNRAS, 269, 837
Bouvier, J., Bertout, C. Benz, W., and Mayor, M., 1986, A&A 165, 110
Bonnell, I.A., Arcoragi, J.-P., Martel, H., Bastien, P. 1992, ApJ., 400, 579
Boss, A. 1993, In *The Realm of Interacting Binary Stars*, eds. J. Sahade, G.E. McCluskey, and Y. Kondo (Dordrecht: Kluwer), p. 335
Cohen, M., and Kuhi, L.V. 1989, ApJS, 41 743
Duchêne, G., Monin, J.-L., Ménard, F., Bouvier, J. 1998, ApJ, in preparation
Dutrey, A., Guiloteau, S., Duvert, G., Prato, L., Simon, M., Schuster, K., Ménard, F. 1996, A&A, 309, 493
Fekel, F.C. 1981, ApJ, 246, 879
Galli, D., Shu, F.H. 1993, ApJ, 417, 220
Ghez, A.M., McCarthy, D.W., Patience, J.L., Beck, T.L. 1997, ApJ, 481, 378
Goodman, A.A., Bastien, P., Myers, P.C., Ménard, F. 1990, ApJ., 359, 363
Hale, A. 1994, AJ, 107, 306
Hartigan, P., Strom, K.M., Strom S.E. 1994, ApJ, 427 961
Hartmann et al., 1986, ApJ, 309, 275
Herbig, G.H., Bell, K.R. 1988, *Third Catalog of Emission-Line Stars of the Orion Population*, Lick Observatory Bulletin No 1111
Kenyon, S.J., and Hartmann, L., 1995, ApJS 101, 117
Larson, R.B. 1995, MNRAS, 272, 213
Mathieu, R.D. 1994, ARA&A, 32, 465
Ménard, F. 1989, Ph.D. Thesis, Univ. of Montréal
Ménard, F., Bastien, P. 1992, AJ, 103, 564
Ménard, F., et al., 1998, in preparation
Moneti, A, Helfer, H.L., McMillan, R.S., Perry, M.L., Pipher, J.L. 1984, ApJ, 282, 508
Osterloh, M., Beckwith, S.V.W. 1995, ApJ, 439, 288
Padgett, D.L., Strom, S.E., Ghez, A. 1997, ApJ, 477, 705
Prato, L., Simon, M., 1997, ApJ, 474, 455
Pringle, J.E. 1989, MNRAS, 239, 361
Redman, R.O., Kuiper, T.B.H., Lorre, J.J., 1986, ApJ 303, 300
Shu, F.H., Adams, F.C., Lizano, S. 1987, ARA&A, 25, 23
Simon, M. 1997, ApJ, 482, L81
Skrutskie, M.F., Dutkevitch, D., Strom, S.E., Edwards, S., Strom, K.M., Shure, M.A., 1990, AJ 99, 1187.
Terquem, C., Bertout, C.M. 1993, A&A,274, 291
Tamura, M., Sato, S. 1989, AJ, 98, 1368
Vrba, F.J., Rydgren, A.E., Chugainov, P.F., and Shakovskaya, N.I., 1989, AJ, 97, 483
Weis, E.W. 1974, ApJ, 190, 331
Whitney, B.A., Hartmann, L. 1992, ApJ, 395, 529
Wood, K., Kenyon, S.J., Whitney, B., and Turnbull, M., 1998, ApJ 497, 404